

1 **Modeling approach to regime shifts of primary production in shallow coastal**
2 **ecosystems**

3 J. M. Zaldívar¹, F.S. Bacelar[†], S. Dueri, D. Marinov, P. Viaroli[§] and E. Hernández-García[†]

4 European Commission, Joint Research Centre, Via E. Fermi 2749,
5 21020-Ispra (VA), Italy

6
7 [†]IFISC, Instituto de Física Interdisciplinar y Sistemas Complejos (CSIC-UIB)
8 Campus Universitat de les Illes Balears, E-07122 Palma de Mallorca, Spain

9
10 [§]Department of Environmental Sciences,
11 University of Parma, Viale G. P. Usberti 33/A, 43100-Parma, Italy

12
13 **Abstract.**

14 Pristine coastal shallow systems are usually dominated by extensive meadows of seagrass species,
15 which are assumed to take advantage of nutrient supply from sediment. An increasing nutrient input is
16 thought to favour phytoplankton, epiphytic microalgae, as well as opportunistic ephemeral macroalgae
17 that coexist with seagrasses. The primary cause of shifts and succession in the macrophyte community
18 is the increase of nutrient load to water; however temperature plays also an important role. A
19 competition model between rooted seagrass (*Zostera marina*), macroalgae (*Ulva sp*), and
20 phytoplankton has been developed to analyse the succession of primary producer communities in these
21 systems. Successions of dominance states, with different resilience characteristics, are found when
22 modifying the input of nutrients and the seasonal temperature and light intensity forcing.

23
24 **Keywords:** regime shifts, macrophytes, macroalgae.

25

¹ Corresponding author. E-mail: jose.zaldivar-comenges@jrc.it; Institute for Health and Consumer Protection, TP272

1. INTRODUCTION

Shallow transitional water systems (McLusky and Elliot. 2007) are intrinsically unstable and highly variable over wide temporal and spatial scales (Kjerfve, 1994; Zaldivar et al., 2008). These ecosystems, being interfaces between terrestrial and aquatic ecosystems, provide essential ecological functions influencing the transport of nutrients, material and energy from land to sea (Wall et al., 2001). Biodiversity can attain low values, but its functional significance remains high (Sacchi, 1995). Therefore, shifts in diversity are likely to have important and profound consequences for ecosystem structure and functioning (Levin et al., 2001). Invasions, competitive advantages, and nonlinear feedback interactions may lead to alternating states and regime shifts (Scheffer et al., 2001) which, once occurred, may pose limits for remediation strategies since it may be difficult, if not impossible, returning to the original state (Webster and Harris, 2004).

Contrary to open seas, where primary production is dominated by phytoplankton, in transitional waters a considerable portion of primary production is performed by angiosperms, epiphytic algae, macroalgae and epibenthic microalgae. In addition, shallow aquatic ecosystems do not show the typical correlation between nutrient inputs and chlorophyll-a in water (Nixon et al., 2001), as already demonstrated for deeper coastal waters and lakes (Vollenweider, 1976).

Regime shift phenomena occurring in shallow coastal areas (Sand-Jensen and Borum, 1991; Nienhuis, 1992; Viaroli et al., 1996; Flindt et al., 1999; Schramm, 1999) have been already documented as the result of the competition between free floating plants and submerged phanerogams.

Several authors have proposed a conceptual scheme that considers nutrient inputs as the main driver in the succession from benthic vegetation to phytoplankton or floating seaweeds in shallow transitional waters (Nienhuis, 1992; Borum, 1996; Valiela et al., 1997; Hemminga, 1998; Nixon et al., 2001). This conceptual scheme is based on the evolution of benthic communities through several phases as the level of nutrients increases. In the pristine stage, the community is dominated by phanerogams species from a relatively small number of genera, i.e. *Zostera*, *Thalassia*, *Halodule*, *Cymodocea*, and *Ruppia*. Nutrient enrichment leads to an increase in epiphytic microalgae, followed by the increase in floating ephemeral macroalgae -as *Ulva* and *Gracilaria*- which compete for light and nutrients thus producing

1 the disappearance of perennial seagrass species. Finally, at high levels of nutrient input, phytoplankton
2 growth increases water turbidity enough to depress macroalgal growth thus leading to a dominance of
3 phytoplankton species.

4 Even though the decline of seagrasses due to anthropogenic eutrophication is a worldwide
5 phenomenon (Orth et al., 2006; Short et al., 2006), there is no direct causality evidence from field data
6 (Ralph et al., 2006). In addition, it is not evident from experimental studies where the limit lies for the
7 dominance shift between these two competing type of organisms are (Schramm, 1999; Hauxwell and
8 Valiela, 2004). Field studies demonstrate that the decrease of seagrass meadows is directly related to
9 nitrogen loadings (Nelson et al., 2003; Hauxwell and Valiela, 2004) and the dominance of macroalgae,
10 especially Ulvae, becomes apparent in eutrophic environments (Borum, 1996). An overview of
11 seagrass responses to nutrient enrichment and/or eutrophication events is presented in Burkholder et al.
12 (2007), whereas the evolution of several Mediterranean coastal lagoons from pristine conditions to the
13 present situation is summarised in Viaroli et al. (2008).

14 Although nutrient loading is one of the main drivers of regime shifts in transitional waters, light and
15 temperature have been also recognised as key abiotic factors controlling algal growth (Schramm,
16 1999). Furthermore, in transitional water ecosystems hydrological and hydrodynamic conditions affect
17 community persistence (Dahlgreen and Kautsky, 2004; Marinov et al., 2007).

18 Regime shifts occurring in shallow aquatic ecosystems were analysed by Scheffer et al. (2003), who
19 developed a minimum model with two ordinary differential equations, one considering floating plants
20 and the other for submerged aquatic vegetation (SAV). Competition between floating vegetation and
21 SAV was found to cause alternate attractors, since floating plants outcompete SAV when light is the
22 only limiting factor, whereas SAV species dominate at low nutrient concentrations since they are able
23 to uptake nutrients from the sediments. The model, although not fully validated with experimental
24 data, was the first to provide a comprehensive explanation of several observed phenomena.

25 In this work, we have studied the regime shifts from SAV to floating macroalgae in shallow brackish
26 ecosystems. We have developed a basic model that accounts for the competition between *Zostera*

1 *marina* and *Ulva* sp. using existing models by Coffaro and Bocci (1997), Bocci et al. (1997) and
2 Solidoro et al. (1997ab). To deal with the ability of seagrass to survive at low nutrient conditions, we
3 have also included the dynamics of inorganic nitrogen (nitrates and ammonium) in the water column
4 and in the sediments (Chapelle, 1995). A simple phytoplankton model (Plus et al., 2003) has been also
5 incorporated in the main model.

6 The integrated model is able to simulate successions of dominance states, with different resilience
7 characteristics according with the conceptual scheme. Regime shifts are found when changing nutrient
8 input, temperature and light intensity forcing functions. Finally, a re-interpretation in terms of
9 sensitivity to initial and operating values is discussed for mesocosm experiments.

10 **2. METHODS**

11 **2.1. Model Formulation**

12 The model is based on previous existing and validated models developed for Mediterranean coastal
13 lagoons, i.e. Venice lagoon (Italy) and Etang de Thau (France). This approach was chosen because it
14 would allow the flexibility of analysing different scenarios for these types of ecosystems which are
15 subjected to strong anthropogenic pressures. In addition, previously validated models can offer more
16 robust results than a “*de novo*” approach when there is no experimental data adequate for their
17 validation.

18 - *Zostera marina* model

19 The *Zostera marina* sub-model is based on the model described in Bocci *et al.* (1997) and Coffaro and
20 Bocci (1997). State variables in this sub-model are: Z_s (shoot biomass, gdw m^{-2}), Z_r (rhizome-root
21 biomass, gdw m^{-2}) and N_z (internal nitrogen quota, mg N gdw^{-1}). *Zostera* growth is described as
22 follows:

$$23 \quad \frac{dZ_s}{dt} = (\text{growth}_z - \text{trans} - \text{respiration}_s) \cdot Z_s \quad (1)$$

$$24 \quad \frac{dZ_r}{dt} = \text{trans} \cdot Z_s - \text{respiration}_r \cdot Z_r \quad (2)$$

$$1 \quad \frac{dN_z}{dt} = uptake_z - growth_z \cdot N_z \quad (3)$$

2 The influence of the limiting factors on *Zostera* growth is described with a multiplicative formulation:

$$3 \quad growth_z = \mu_{max}^z \cdot f_1(I) \cdot f_2(T) \cdot f_3(N_z) \cdot f_4(Z_s) \cdot f_5(NO_3^-) \quad (4)$$

4 The functional forms as well as the parameters of the model are described in Table 1. The f_5 term has
 5 been introduced in the Bocci et al. (1997) model to take into account that water-column nitrate
 6 enrichment promotes decline of *Zostera marina* independently of algal light attenuation. According to
 7 Burkholder et al. (1992) this is probably due to internal imbalances in nutrient supply ratios.

8 In this formulation, the growth of rhizome depends on the translocation of photosynthetic products
 9 from leaves to below-ground parts of the plant. This translocation is proportional to the rate of growth:

$$10 \quad trans = K_{trans} \cdot growth_z \quad (5)$$

11 The parameter K_{trans} was estimated by Olsen and Sand-Jensen (1993) as 25% of the growth, i.e.
 12 $K_{trans}=0.25$. Shoot biomass losses are expressed as a function of shoot respiration rate at 20 °C, SR_{20} ,
 13 corrected by the actual temperature:

$$14 \quad respiration_s = SR_{20} \cdot f_s(T) \quad (6)$$

15 where

$$16 \quad f_s(T) = 0.098 + \exp(-4.690 + 0.2317 \cdot T) \quad (7)$$

17 Following a similar approach, rhizome-root biomass loss processes are considered as a function of a
 18 respiration coefficient, RR_{20} , with a temperature correction:

$$19 \quad respiration_r = RR_{20} \cdot f_r(T) \quad (8)$$

20 Internal nitrogen quota in *Zostera* has been modelled as a function of nitrogen uptake. Shoots can
 21 uptake nitrates and ammonium, whereas the rhizome-root can only uptake ammonium.

$$22 \quad uptake_z = (uptake_s + uptake_r) \cdot f_u(N_z) \quad (9)$$

$$23 \quad uptake_s = uptake_s^{NH_4^+} + uptake_s^{NO_3^-} \quad (10)$$

$$24 \quad uptake_s^{NH_4^+} = V_{max_s}^{NH_4^+} \frac{[NH_4^+]}{[NH_4^+] + K_s^{NH_4^+}} \quad (11)$$

$$1 \quad uptake_s^{NO_3^-} = V_{max_s}^{NO_3^-} \frac{[NO_3^-]}{[NO_3^-] + K_s^{NO_3^-}} \quad (12)$$

$$2 \quad uptake_r = V_{max_r}^{NH_4^+} \frac{[NH_4^+]_s}{[NH_4^+]_s + K_r^{NH_4^+}} \quad (13)$$

$$3 \quad f_u(Nz) = \frac{Nz_{max} - Nz}{Nz_{max} - Nz_{min}} \quad (14)$$

4 The values of parameters are summarised in Table 1.

5 - Ulva rigida model

6 The *Ulva rigida* sub-model is based on the model described in Solidoro *et al.* (1997a,b). State
 7 variables in this sub-model are: U (*Ulva* biomass, gdw l⁻¹) and Nu (internal nitrogen quota, mg N gdw⁻¹).
 8 The model can be written as:

$$9 \quad \frac{dU}{dt} = (growth_u - death_u) \cdot U \quad (15)$$

10 The influence of the limiting factors on *Ulva* growth was described with a multiplicative formulation:

$$11 \quad growth_u = \mu_{max}^u \cdot g_1(I) \cdot g_2(T) \cdot g_3(Nu) \quad (16)$$

12 The functional forms of the algae model are described in Table 2. As we do not consider oxygen
 13 dynamics explicitly, the mortality in this model does not follow Solidoro *et al.* (1997a,b) model. In this
 14 case, the mortality term has been expressed as a simple constant and a density dependent function:

$$15 \quad death_u = k_d^u + k_t^u \cdot \exp\left[-\left(\frac{U - U_{max}}{U_{width}}\right)^2\right] \quad (17)$$

16 Like *Zostera marina*, *Ulva* is able to store nitrogen, therefore Solidoro *et al.* (1997a,b) introduced the
 17 tissue concentration of this element (Nu) as a separated state variable. Its dynamics can be expressed
 18 as:

$$19 \quad \frac{dNu}{dt} = uptake_u - growth_u \cdot Nu \quad (18)$$

20 The specific uptake rate of nitrogen depends on the chemical form available and on the level Nu of
 21 nitrogen tissue concentration. Hence, *uptake* can be written as

$$1 \quad uptake_u = (uptake_u^{NH_4^+} + uptake_u^{NO_3^-}) \cdot f_u(Nu) \quad (19)$$

2 whereas

$$3 \quad uptake_u^{NH_4^+} = V_{max_u}^{NH_4^+} \frac{[NH_4^+]}{[NH_4^+] + K_u^{NH_4^+}} \quad (20)$$

$$4 \quad uptake_u^{NO_3^-} = V_{max_u}^{NO_3^-} \frac{[NO_3^-]}{[NO_3^-] + K_u^{NO_3^-}} \quad (21)$$

$$5 \quad f_u(Nu) = \frac{Nu_{max} - Nu}{Nu_{max} - Nu_{min}} \quad (22)$$

6 - Phytoplankton model

7 A simple phytoplankton module was introduced in the model. The module, developed for Etang de
 8 Thau (France), has been adapted from Plus et al. (2003). Phytoplankton will compete for nutrients in
 9 the water column and will have a shadowing effect - less pronounced than that of *Ulva*- on benthic
 10 vegetation.

$$11 \quad \frac{dP}{dt} = (growth_p - death_p) \cdot P \quad (23)$$

12 The influence of the limiting factors on phytoplankton growth was described with a multiplicative
 13 formulation (Plus et al., 2003):

$$14 \quad growth_p = \mu_{max}^P \cdot h_1(I) \cdot h_2(T) \cdot h_3(N) \quad (24)$$

15 whereas mortality is also described as a function of temperature:

$$16 \quad death_p = m_0 \cdot e^{\varepsilon \cdot T} \quad (25)$$

17 As we do not explicitly consider zooplankton grazing explicitly, the mortality function in this model
 18 has been changed accordingly. Phytoplankton nutrient uptake can be expressed as a function of the
 19 nutrient limitation expression and phytoplankton biomass as in Plus et al., (2003). The functional
 20 forms of the phytoplankton growth model as well as the main parameters are described in Table 3.

21 - Dissolved Inorganic Nitrogen (DIN) model

22 To model the competition between *Zostera* and *Ulva* it is necessary to include nutrient consumption.
 23 The nutrients included are nitrogen in the oxidised and reduced forms. Furthermore, in shallow water

1 bodies, sediments play a fundamental role in the nutrient dynamics and in this case *Zostera* is able to
 2 uptake ammonium from sediments (Coffaro and Bocci, 1997). For these reasons, the dynamics of DIN
 3 in sediments has been introduced as well. The model, adapted from Chapelle (1995), can be written as:

4 *a/ Dissolved Inorganic Nitrogen (DIN) in the water column*

$$5 \frac{d[NO_3^-]}{dt} = Nitrif_w - uptake^{NO_3^-} + \frac{Q_{NO_3^-}^{diffusion}}{watervol} + Q_{NO_3^-}^{input} - Q_{NO_3^-}^{output} \quad (26)$$

$$6 \frac{d[NH_4^+]}{dt} = -Nitrif_w - uptake^{NH_4^+} + \frac{Q_{NH_4^+}^{diffusion}}{watervol} + Q_{NH_4^+}^{input} - Q_{NH_4^+}^{output} \quad (27)$$

7 Nitrification rates in the water column are functions of water temperature and oxygen concentration,
 8 and they can be expressed as:

$$9 Nnitrif_w = k_{nit} \cdot \exp(k_t \cdot T) \cdot [NH_4^+] \quad (28)$$

10 $[NO_3^-]$ uptake ($mmol N \cdot m^{-3} \cdot h^{-1}$) can be divided into *Ulva*, *Zostera* and phytoplankton uptake:

$$11 uptake^{NO_3^-} = \alpha_1 \cdot (uptake_u^{NO_3^-} + uptake_z^{NO_3^-}) + uptake_p^{NO_3^-} \quad (29)$$

12 whereas α_l is a conversion factor to pass from mg N to mmol N.

13 $[NH_4^+]$ uptake ($mmol N \cdot m^{-3} \cdot h^{-1}$) can also be divided into *Ulva*, *Zostera* and phytoplankton uptake:

$$14 uptake^{NH_4^+} = \alpha_1 \cdot (uptake_u^{NH_4^+} + uptake_z^{NH_4^+}) + uptake_p^{NH_4^+} \quad (30)$$

15 At the interface between the water column and the interstitial water, diffusion is responsible for

16 $[NO_3^-]$ and $[NH_4^+]$ fluxes ($mmol N \cdot m^{-3} \cdot h^{-1}$). These fluxes can be represented as:

$$17 Q_{NO_3^-}^{diffusion} = D_{NO_3^-} \frac{A \cdot \beta}{z_s} ([NO_3^-]_s - [NO_3^-]) \quad (31)$$

$$18 Q_{NH_4^+}^{diffusion} = D_{NH_4^+} \frac{A \cdot \beta}{z_s} ([NH_4^+]_s - [NH_4^+]) \quad (32)$$

19 whereas D_X are the sediment diffusion coefficients ($m^2 h^{-1}$), A is the exchange area ($1 m^2$), z_s is the
 20 distance between the centres of the water and sediment layers, and β is the sediment layer porosity
 21 (Chapelle, 1995).

1 This DIN submodel behaves as a CSTR (Continuous Stirred Tank Reactor), where the forcing is given
 2 by the fluxes of nutrients. For example, for nitrate it can be written:

$$3 \quad Q_{NO_3^-}^{input} = \frac{F \cdot [NO_3^-]_{initial}}{V} \quad (33)$$

$$4 \quad Q_{NO_3^-}^{output} = \frac{F \cdot [NO_3^-]}{V} \quad (34)$$

5 where F refers to the water flow (m^3/h), V to the total volume ($1 m^3$) and $[NO_3^-]_{initial}$ is the initial
 6 concentration of nitrate that enters into the system.

7 *b/ DIN in the sediments*

$$8 \quad \frac{d[NO_3^-]_s}{dt} = Nitrif_s - Ndenit - \frac{Q_{NO_3^-}^{diffusion}}{interstvol} \quad (35)$$

$$9 \quad \frac{d[NH_4^+]_s}{dt} = (1 - \alpha_{denit})Ndenit - Nitrif_s - uptake_r - \frac{Q_{NH_4^+}^{diffusion}}{interstvol} \quad (36)$$

10 Nitrification in the sediments, $Nitrif_s$, can be described as a first order process in ammonium
 11 concentration at the sediment:

$$12 \quad Nnitrif_s = k_{nit} \cdot f_1(T) \cdot f_2(O) \cdot [NH_4^+]_s \quad (37)$$

13 whereas nitrate reduction can be expressed as a first order process in nitrate concentration at the
 14 sediment:

$$15 \quad Ndenit = k_{denit} \cdot f_1(T) \cdot f_3(O) \cdot [NO_3^-]_s \quad (38)$$

16 Nitrogen mineralization has not been taken into account in this model. Oxygen concentration is
 17 considered constant. The values of parameters taken from Chapelle (1995) are summarised in Table 4.

18 **2.2. Forcing functions and parameters**

19 In all the runs, the model has been forced by imposing temperature and solar radiation sinusoidal
 20 forcing, which have the following form:

$$21 \quad T = A_T \cdot \sin\left(2 \cdot \pi \left(\frac{t - 114.74}{365}\right)\right) + T_m \quad (39)$$

$$I = A_I \cdot \left[\sin \left(2 \cdot \pi \left(\frac{t - 90}{365} \right) \right) + 1 \right] + I_m \quad (40)$$

Parameters, amplitude and mean value, were adjusted using meteorological data from several Mediterranean stations, but, in any case, their influence is going to be analyzed.

Nutrient inputs and flows have been maintained constant during each simulation run. This is not typical under natural conditions where nutrient loadings delivered to coastal systems undergo seasonal variations due to rainfall regimes. In addition in the Mediterranean climate region, nutrient loadings to coastal marine systems can attain short term peaks following heavy rainfall events (Plus et al., 2006). Furthermore, oxygen concentrations were set constant at 8.0 g m⁻³ during all simulations, whilst in transitional water ecosystems they undergo daily and seasonal variations from supersaturation to anoxia (Viaroli and Christian, 2003).

2.3. Assessment of mesocosm data

Mechanistic experiments dealing with phanerogams-macroalgae-phytoplankton competition were carried out using mesocosms under controlled conditions (Taylor et al., 1999; Nixon et al., 2001). In this work we have re-assessed the mesocosms experiments reported by Taylor et al. (1999). In these experiments (five settings, each with two replicates: Control, C, Low, L, Medium, M, High, H and Very High, VH) enrichment with ammonium and phosphate at several levels was performed and results monitored from April to September.

The following assumptions were made to simulate these experiments:

- Light intensity was assumed to be not a limiting factor for any of the three taxa.
- Temperature was simulated using a sinusoidal function as in Eq. (39) with $T_m=10.5$ and $A_T=10.1$ °C, respectively.
- Dissolved inorganic phosphorous (DIP) was not considered.
- Dissolved inorganic nitrogen (DIN) was equally partitioned between nitrates and ammonium in the background concentration.
- Initial conditions of *Zostera* above-ground biomass were taken constant at 50 gdw m⁻² whereas the influence of initial conditions of *Ulva* and phytoplankton was assessed.

1 - A constant flow, $F=5.3 \cdot 10^{-3} \text{ m}^3 \text{ h}^{-1}$ was assumed during all the experiment, as well as a constant
2 concentration input of nitrate, $[NO_3^-]_{input} = 2.4 \text{ mmol m}^{-3}$ and ammonium, $[NH_4^+]_{input} = 2.4, 20.6, 38.7,$
3 $75.1, 148.0 \text{ mmol m}^{-3}$, for the different experimental conditions (C, L, M, H and VH).

4 **3. RESULTS**

5 **3.1. Competition between *Zostera* and *Ulva***

6 The first set of simulations was run excluding phytoplankton, to compare with field observations for
7 which no phytoplankton data was mentioned. At low DIN input concentrations (5 mmol m^{-3}) *Zostera*
8 survives and *Ulva* disappears (Fig. 1). In addition, due to the relatively high flow of DIN into the
9 system, nitrogen is not completely depleted and the dynamics in the water column and in the sediments
10 are tightly coupled. However, there is a certain transient period of few years before the limit cycle is
11 reached, during which both vegetation types coexist.

12 The contrary effect, i.e. dominance by *Ulva*, may be observed at high input DIN concentrations (50
13 mmol m^{-3} , see Fig. 2). Keeping high nutrient loads, *Zostera* will disappear after a few years while *Ulva*
14 will tend to prevail.

15 In order to analyze the effects of DIN inputs in the *Zostera-Ulva* competition model, we have run the
16 model for a set of flow conditions with the same forcing. Figures 3 and 4 present the results in terms of
17 average biomass over the year. *Zostera* dominates the regions with low DIN concentrations whereas
18 the opposite applies to *Ulva*. In addition, due to the fact that in the *Zostera* model the rhizome-root is
19 assumed to only uptake ammonium (Bocci et al, 1997), there is an asymmetry concerning the effects
20 ammonium and nitrate in the figures. Since we consider explicitly the DIN dynamics, the results
21 represented in Figs. 3 and 4 will change as a function of the flow ($F, \text{m}^3 \cdot \text{h}^{-1}$), assuming the same initial
22 concentrations of nutrients. Likely, at low flows depletion of DIN may occur in the water column as
23 well as in the sediments during the periods of maximum growth. This affects the dynamics in the
24 system and, consequently, the competition between the two taxa. In order to highlight these
25 differences, we have plotted the results obtained with 0.1 and $0.01 \text{ m}^3 \cdot \text{h}^{-1}$ flows.

1 To verify the sensitivity of the competition in relation to changes in temperature, several simulations
2 were set up, with the same conditions as in Fig.1, but with average temperature increased from 0.2 to 2
3 °C. Results obtained for a temperature increase of 1 °C after the fifth year are presented in Figure 5. In
4 this case, the outcome is the opposite as in Fig. 1 with *Ulva* dominating the competition. Dynamics and
5 timing of the regime shift are not a simple function of the temperature increase, as shifts have been
6 observed in all the temperature ranges studied depending on the initial and forcing conditions.

7 The model was also run changing mean temperatures (T_m) and annual temperatures (A_T) ranges, Eq.
8 (39). Results are presented in Fig. 6, showing that an increase of both parameters tends to favor *Ulva*
9 growth, even in environments with low nutrient concentrations.

10 Finally the results of the model were analyzed as a function of the incident light. A series of simulation
11 were run by modifying the average light intensity (I_m) and its annual range (A_I), see Eq. (40). From the
12 results presented in Fig.7 it can be inferred that *Zostera* is adapted to narrower light ranges while *Ulva*
13 seems able to cope with high variable light regimes (Dahlgreen and Kautsky, 2004). However, there is
14 a certain realm of lighting conditions within which *Zostera* dominates even at high DIN
15 concentrations. All simulated results showed that the system was in a transient and the final limit cycle
16 was reached after a few years.

17 **3.2. The influence of phytoplankton on competition between *Zostera* and *Ulva***

18 The partitioning of primary production among the different taxa was analyzed under different set of
19 conditions as a function of DIN inputs with high ($F=0.1 \text{ m}^3 \text{ h}^{-1}$) and low flows ($F=0.01 \text{ m}^3 \text{ h}^{-1}$), see Fig.
20 8. Overall, phytoplankton was able to compete with *Ulva* for nutrients in the water column, thus
21 favouring *Zostera* due to its lower shadowing effect. At high DIN loadings phytoplankton
22 outcompeted both *Ulva* and *Zostera*, thus becoming the dominant group. This is due to its higher
23 maximum growth rate (0.021 h^{-1}) compared to *Ulva* (0.017 h^{-1}) and *Zostera* (0.0025 h^{-1}) when no
24 nutrient, temperature or light limitation exists.

25 **3.3. Assessment of mesocosm experiments**

1 The model has been used to simulate the mesocosm experiments which tested competition between
2 *Zostera marina*, *Ulva lactuca* and phytoplankton under several nutrient enrichment conditions (Taylor
3 et al., 1999; Nixon et al., 2001). The authors concluded that no significant effect of loading could be
4 detected for *Zostera marina*, epiphytic material, drift macroalgae or for all plant components
5 combined. This contradictory result could be due to several reasons; therefore in this work we have
6 tried to assess two: sensitivity to initial conditions and transient behaviour.

7 Concerning the sensitivity to initial conditions, results obtained from two identical runs of the
8 mesocosm experiments, but with different initial biomass of *Ulva* and phytoplankton are reported in
9 Figures 9 and 10, as an example. In the first case, *Zostera* biomasses increased steadily with nutrient
10 enrichment, from C to M and decreased from M and VH. In parallel, *Ulva* and phytoplankton
11 increased with nutrient enrichment from C to VH (Fig. 9). However, in the second case (Fig. 10), even
12 though *Ulva* and phytoplankton behaved in a similar way but with delayed dynamics and with
13 different values, *Zostera* showed a different behaviour with higher biomasses at higher concentrations.

14 **4. DISCUSSION**

15 The simulated results from the competition between *Zostera* and *Ulva* are in agreement with field
16 observations. For example, DIN concentrations around 5 mmol m^{-3} are typical from Etang de Thau
17 (France), which is covered by *Zostera* meadows; whereas high DIN concentrations $\sim 50 \text{ mmol m}^{-3}$
18 have occurred during some years in Sacca di Goro. (Italy), which is dominated by *Ulva*. Similar
19 observations have also been reported by Nelson et al. (2003) with *Ulva* starting to appear at DIN
20 concentrations higher than 18.0 mmol m^{-3} . However, the regime shift would be more abrupt since,
21 with such high *Ulva* biomasses, *Zostera* would disappear not only due to nutrient competition, but also
22 due to alteration of sediment biogeochemistry (Holmer et al., 2003) and anoxic crises triggered off by
23 the biomass decomposition (Zaldívar et al., 2003).

24 Biomasses and *Ulva-Zostera* competition are more correlated with DIN loads than with mean DIN
25 concentrations, since with high growth rates nutrients become depleted. This is one of the reasons why
26 field observations are difficult to use for defining a regime shift value.

1 Simulation outcomes evidenced that system responses to DIN loadings are complex depending on
2 multiple parameters. For example, environmental conditions, such as temperature and light intensity,
3 seem to play an important role in controlling the competition between benthic and pelagic species.
4 Therefore, attempts to develop a simple nutrient scale for detecting regime shift in benthic vegetation
5 seems not possible. This is probably one of the reasons why experimental observations and mesocosm
6 data do not provide a clear threshold/range of values for regime shifts.

7 The results of simulations considering the influence of temperature and light intensity can be
8 informative on climatic conditions and depths at which *Zoostera* is able to grow when competing with
9 *Ulva* by providing plausible values at which regime shifts will occur. The simulations can also help the
10 debate on how changes in incident light's spectrum and intensity would affect the benthic vegetation.

11 The simulation of mesocosm experiments highlighted that the model of benthic vegetation is very
12 sensitivity to initial (biomass concentrations) and operating (temperature, light intensity, DIN flows)
13 conditions. Such result is in agreement with high variability detected in data, where biomasses differed
14 by a factor of two between the experimental replicates (Taylor et al., 1999). In addition, transient
15 regimes last longer (years) than the duration of the experiments (months); therefore, results could be
16 not adequate to demonstrate the effects of nutrient enrichment on plant competition. Differences could
17 be amplified by manipulations, e.g. when setting mesocosms with sediment transfer and phanerogams
18 transplanting.

19 **5. CONCLUSIONS**

20 In this work a competition model has been developed with the aim of analysing the succession of
21 primary producer communities in coastal shallow ecosystems and identifying possible nutrient
22 thresholds which cause shifts between alternative stable states.

23 The integrated model is able to simulate succession of dominance states, with different resilience
24 characteristics according with the conceptual scheme that sees floating macroalgae as the optimal
25 competitors for light, and submerged phanerogams as most efficient in recovering and storing nutrients
26 from the sediments and from the water column. The shift from phanerogams to macroalgae, and finally

1 to phytoplankton dominated communities, conformed to the general theory of succession in coastal
2 lagoons (Viaroli et al., 2008). Field observations support the view that in nutrient poor ecosystems,
3 rizophytes dominate until they are not limited by light penetration (depth effect) or by turbidity and
4 shading by floating vegetation and phytoplankton (Dahlgreen and Kautsky, 2004). Increasing loading
5 rates support the development of macroalgae, whilst high loaded water masses become dominated by
6 phytoplankton.

7 Regime shifts are found when changing the input of nutrients, but also, model simulations were
8 sensitive to environmental forcing: temperature and light.

9 Overall, model runs evidenced a clear tendency towards a shift from seagrass to macroalgae under
10 increasing temperatures. However, it is expected that the occurrence and severity of the shifts will be
11 site specific depending on local conditions and past history. These results point out that one of the
12 possible outcomes of an average air temperature increase will be the increase in macroalgae and
13 decrease in benthic vegetation. However, the results of the analysis of a competition model between
14 two species are not sufficient to sustain this point.

15 The model shows a high sensitivity to initial conditions as well as to forcing parameters, but this effect
16 is also observed in mesocom experiments (Taylor et al., 1999). Furthermore, model simulations show
17 that, when initial conditions do not correspond to steady state conditions, seagrasses communities
18 require time periods to attain steady state, which usually are longer than the duration of the mesocosm
19 experiments. In addition, ecosystems, as other non-linear dynamical systems, are sensitive to initial
20 conditions and even a small difference may drive the system to a completely different position in state
21 space after a certain time (Pahl-Wostl, 1995). Our results suggest that this is probably the main reason
22 behind the high variability found by Taylor et al. (1999) in their experiments, which did not allow
23 finding a clear correlation between nutrient increase and regime shifts.

24 In its present form, the model does not take into consideration several important aspects such as
25 hydrodynamics, buffering capacity (De Wit et al., 2001; Viaroli et al., 2008), salinity, organic nutrient,
26 oxygen, zooplankton and bacteria as well as interactions between *Ulva* and aquaculture activities. In

1 order to develop a more realistic assessment of regime shifts in terms of range of concentrations and
2 temperature, we plan to consider a real case study in which the studied taxa coexist. Future efforts will
3 aim to implement the competition model using a 3D hydrodynamic approach such as COHERENS
4 (Luyten et al., 1999) for Thau lagoon (France).

5

6 **Acknowledgements.** This research has been partially supported by the THRESHOLDS (FP6
7 Integrated Project Thresholds of Environmental Sustainability, contract n° 003933) and the DITTY
8 (FP5 Energy, Environment and Sustainable Development Programme EVK3-CT-2002-00084)
9 projects. F.S.B. and E.H.-G. acknowledge also support from Spanish MEC and FEDER through the
10 project FISICOS (FIS2007-60327).

11

1 REFERENCES

- 2 Bocci M, Coffaro G. and Bendoricchio G., 1997. Modelling biomass and nutrient dynamics in eelgrass
3 (*Zostera marina* L.): applications to the Lagoon of Venice (Italy) and Oresund (Denmark) *Ecol.*
4 *Model.* 102, 67-80.
- 5 Borum J, 1996. Shallow waters and land/sea boundaries. *Coastal and Estuarine Studies* 52, 179-203.
- 6 Burkholder J. M., Tomasko, D. A. and Touchette B. W. 2007. Seagrasses and eutrophication. *Journal*
7 *of Experimental Marine Biology and Ecology* 350, 46-72.
- 8 Burkholder, A. M., Mason, K. M., Glasgow Jr. H. B., 1992. Water-column nitrate enrichment
9 promotes decline of eelgrass *Zostera Marina*: evidence from seasonal mesocosm experiments.
10 *Mar. Ecol. Prog. Ser.* 81, 163-178.
- 11 Chapelle, A., 1995. A preliminary model of nutrient cycling in sediments of a Mediterranean lagoon.
12 *Ecol. Model.* 80, 131-147.
- 13 Coffaro G. and Bocci M., 1997. Resources competition between *Ulva rigida* and *Zostera marina*: a
14 quantitative approach applied to the Lagoon of Venice. *Ecol. Model.* 102, 81-95.
- 15 Dahlgreen S, Kautsky L, 2004. Can different vegetative states in shallow coastal bays of the Baltic Sea
16 be linked to internal nutrient levels and external nutrient loads? *Hydrobiologia* 514: 249-258.
- 17 Flindt MR, Pardal MA, Lillebø AI, Martins I, Marques JC, 1999. Nutrient cycling and plant dynamics
18 in estuaries: a brief review. *Acta Oecologica* 20, 237-248.
- 19 Hauxwell J, Valiela I, 2004. Effects of nutrient loading on shallow seagrass-dominated coastal
20 systems: patterns and processes. In Nielsen SL, Banta GT, Pedersen MF (eds), *Estuarine nutrient*
21 *cycling: the influence of primary producers*. Kluwer Academic Publishers, Dordrecht, The
22 Netherlands: 59-92.
- 23 Hemminga MA, 1998. The root/rhizome system of seagrasses: an asset and a burden. *Journal of Sea*
24 *Research* 39, 183-196.
- 25 Holmer M, Duarte C.M., Marbà N, 2003. Sulphur cycling and seagrass (*Posidonia oceanica*) status in
26 carbonate sediments. *Biogeochemistry* 66: 223-239.
- 27 Kjerfve, B., 1994. *Coastal Lagoon Processes*. Elsevier Science Publishers, Amsterdam, xx + 577 pp.
- 28 Levin, L.A., Boesch, D.F., Covich, A., Dahm, C., Erséus, C., Ewel, K. C., Kneib, R.T., Moldenke, A.,
29 Palmer, M.A., Snelgrove, P., Strayer, D. and Weslawski, J. M. 2001. The function of marine
30 critical transition zones and the importance of sediment biodiversity. *Ecosystems* 4, 430-451.
- 31 McLusky, D.S. and Elliott, M. 2007. Transitional waters: A new approach, semantics or just muddying
32 the waters? *Estuarine, Coastal and Shelf Science* 71, 359-363.
- 33 Marinov, D. Galbiati, L., Giordani, G., Viaroli, P., Norro, A., Bencivelli, S. and Zaldívar J.M., 2007,
34 An integrated modelling approach for the management of clam farming in coastal lagoons.
35 *Aquaculture* 269, 306-320.

- 1 Nelson, T.A., Nelson A.V. and Tjoelker, M. 2003. Seasonal and spatial patterns of “Green
2 tides”(Ulvoid algal blooms) and related water quality parameters in the coastal waters of
3 Washington State, USA. *Botanica Marina* 46, 263-275.
- 4 Nienhuis PH, 1992. Ecology of coastal lagoons in the Netherlands (Veerse Meer and Grevelingen).
5 *Vie et Milieu* 42, 59-72.
- 6 Nixon, S., Buckley, B., Granger, S. and Bintz, J., 2001. Responses of very shallow marine ecosystems
7 to nutrient enrichment. *Human and Ecological Risk Assessment* 7, 1457-1481.
- 8 Olesen B. and Sand-Jensen K, 1993. Seasonal acclimatation of eelgrass *Zostera marina* growth to light.
9 *Marine. Ecology Progress Series* 94, 91-99.
- 10 Orth, R.J., Carruthers, T.J.B., Dennison, W.C., Duarte, C.M., Fourqurean, J.W, Heck, K.L. Hughes,
11 A.R., Kendrick, G. A., Kenworthy, W.J., Olyarnik, S., Short, F.T., Waycott, M. and Williams, S.
12 L. 2006. A global crisis for seagrass ecosystems. *BioScience* 56, 987-996.
- 13 Pahl-Wostl, C. 1995. The dynamic nature of ecosystems: Chaos and order entwined. Wiley, pp 280.
- 14 Plus, M., Chapelle, A., Lazure, P., Auby, I., Levavasseur, G., Verlaque, M., Belsher, T., Deslous-Paoli,
15 J.M., Zaldívar, J.M. and Murray, C.N. 2003. Modelling of oxygen and nitrogen cycling as a
16 function of macrophyte community in the Thau lagoon. *Continental Shelf Research* 23, 1877-1898.
- 17 Plus, M., La Jeunesse, I., Bouraoui, F., Zaldívar, J. M., Chapelle, A., and Lazure, P., 2006. Modelling
18 water discharges and nutrient inputs into a Mediterranean lagoon. Impact on the primary
19 production. *Ecol. Model.* **193**, 69-89.
- 20 Ralph, P.J., Tomasko, D., Moore, K., Seddon, S. and Macinnis-Ng, C. M. O., 2006. Human impacts on
21 seagrasses: eutrophication, sedimentation and contamination. In: Larkum, A. W. D., Orth, R. J.,
22 Duarte, C. M. (Eds.), *Seagrasses: Biology, Ecology and Conservation*. Springer. The Netherlands,
23 pp. 567-593.
- 24 Sacchi, C. F. ,1995. Le lagune costiere come ambienti di transizione. *Atti VI Congresso Nazionale*
25 *S.It.E.* **16**, 149–154
- 26 Sand-Jensen K. and Borum J, 1991. Interactions among phytoplankton, periphyton, and macrophytes
27 in temperate freshwater and estuaries. *Aquatic Botany* 41, 137-175.
- 28 Scheffer M., Carpenter S., Foley J.A., Folke C. and Walker B., 2001. Catastrophic shifts in
29 ecosystems. *Nature* 413, 591–596.
- 30 Scheffer, M., Szabó, S., Gragnani, A., van Nes E. H., Rinaldi, S., Kautsky, N., Norberg, J., Roijackers,
31 R.M.M. and Franken, R.J.M. 2003. Floating plant dominance as a stable state. *Proc. Nat. Acad.*
32 *Sci.* 100, 4040-4045.
- 33 Schramm W, 1999. Factors influencing seaweed responses to eutrophication: some results from EU-
34 project EUMAC. *Journal of Applied Phycology* 11, 69-78.

- 1 Short, F. T., Koch, E.W., Creed, J. C., Magalhaes Fernandez, E. and Gaeckle, J.L. 2006. SeagrassNet
2 monitoring across the Americas: case studies of seagrass decline. *Mar. Ecol.* 27, 277-289.
- 3 Solidoro, C., Brando, V. E., Dejak, C., Franco, D., Pastres, R., Pecenik, G., 1997a. Long term
4 simulations of population dynamics of *Ulva r.* in the lagoon of Venice. *Ecol. Model.* 102, 259-272.
- 5 Solidoro, C., Pecenik, G., Pastres, R., Franco, D. and Dejak, C., 1997b. Modelling macroalgae (*Ulva*
6 *rigida*) in the Venice lagoon: Model structure identification and first parameters estimation. *Ecol.*
7 *Model.* 94, 191-206.
- 8 Taylor, D.I., Nixon, S.W., Granger, S. L. and Bu Kley, B.A. 1999. Responses of coastal lagoon plant
9 communities to levels of nutrient enrichment: A mesocosm study. *Estuaries* 22, 1041-1056.
- 10 Touchette, B.W., Burkholder, J.M. and Glasgow, H. B. 2003. Variations in eelgrass (*Zostera Marina*
11 L.) morphology and internal nutrient composition as influenced by increased temperature and
12 water column nitrate. *Estuaries* 26, 142-155.
- 13 Valiela I, McLelland J, Hauxwell J, Behr PJ, Hersh D, Foreman K, 1997. Macroalgal blooms in
14 shallow estuaries: controls and ecophysiological and ecosystem consequences. *Limnology and*
15 *Oceanography* 42, 1105-1118.
- 16 Viaroli P, Bartoli M, Bondavalli C, Christian RR, Giordani G, Naldi M, 1996. Macrophyte
17 communities and their impact on benthic fluxes of oxygen, sulphide and nutrients in shallow
18 eutrophic environments. *Hydrobiologia* 329, 105-119.
- 19 Viaroli P, Christian RR, 2003. Description of trophic status of an eutrophic coastal lagoon through
20 potential oxygen production and consumption: defining hyperautotrophy and dystrophy. *Ecological*
21 *Indicators* 3, 237-250.
- 22 Viaroli, P., Bartoli, M., Giordani, G., Naldi, M., Orfanidis, S. and Zaldívar, J.M., 2008. Community
23 shifts, alternative stable states, biogeochemical controls and feedbacks in eutrophic coastal
24 lagoons: a brief overview. *Aquatic Conservation Freshwater and Marine Ecosystems* 18, S105-
25 S117.
- 26 Vollenweider R. A., 1976. Advances in defining critical loading levels for phosphorous in lake
27 eutrophication. *Mem. Ist. Ital. Idrobiol.* 33, 53-83.
- 28 Wall, D. H., Palmer, M. A. and Snelgrove, V. R., 2001. Biodiversity in critical transition zones
29 between terrestrial, freshwater and marine soils and sediments: Processes, linkages, and
30 management implications. *Ecosystems* 4, 418-420.
- 31 Webster. I. T. and Harris, G. P., 2004. Anthropogenic impacts on the ecosystems of coastal lagoons:
32 modelling fundamental biogeochemical process and management implications. *Marine and*
33 *freshwater research* 55, 67-68.

- 1 Zaldívar, J. M., Cattaneo, E., Plus, M., Murray, C. N., Giordani, G. and Viaroli, P., 2003, Long-term
2 simulation of main biogeochemical events in a coastal lagoon: Sacca di Goro (Northern Adriatic
3 Coast, Italy). *Continental Shelf Research* 23, 1847-1876.
- 4 Zaldívar, J.M., Cardoso, A.C., Viaroli, P., Newton, A., de Wit, R., Ibañez, C., Reizopoulou, S.,
5 Somma, F., Razinkovas, A., Basset, A., Holmer, M. and Murray, N. 2008. Eutrophication in
6 transitional waters: An overview. *Transitional Waters Monographs* (in press).
- 7

TABLES AND FIGURES

Table 1. Parameters and computed quantities used in the *Zostera marina* model from Bocci *et al.* (1997) and Coffaro and Bocci (1997).

Parameters, computed quantities	Description	Value
μ_{\max}^z	Maximum specific growth,	0.0025 h ⁻¹
$f_1(I)$	$f_1(I) = \frac{I}{I + K_I^z}$	
K_I^z	Semisaturation constant for light	500 Kcal m ⁻² d ⁻¹
	$I = I_0 \exp[-(\varepsilon_w + \varepsilon_u \cdot U)z]$	
ε_w	Water extinction coefficient	0.4 m ⁻¹
ε_u	Ulva shading coefficient	40 l gdw ⁻¹ m ⁻¹
$f_2(T)$	$f_2(T) = \exp\left[-\left(\frac{T - T_{opt}^z}{T_{width}^z}\right)^2\right]$	
T_{opt}^z	Optimal temperature	20 °C
T_{width}^z	Temperature range, sigmoid width	3.6 °C
$f_3(Nz)$	$f_3(Nz) = \frac{Nz - Nz_{\min}}{Nz_{crit} - Nz_{\min}}$	
Nz_{\min}	Minimum internal nitrogen quota	5.0 mg N gdw ⁻¹
Nz_{\max}	Maximum internal nitrogen quota	30.0 mg N gdw ⁻¹
Nz_{crit}	Critical internal nitrogen quota	15.0 mg N gdw ⁻¹
$f_4(Zs)$	$f_4(Zs) = 1 - \exp\left[-\left(\frac{Zs - Zs_{\max}}{Zs_{width}}\right)^2\right]$	
Zs_{\max}	Maximum shoot biomass	500 gdw m ⁻²
Zs_{width}	Growth dependence on space availability	5 gdw m ⁻²
	$f_5(NO_3^-) = \exp\left[-\left(\frac{NO_3^- - NO_{3_{opt}}^-}{NO_{3_{width}}^-}\right)^2\right]$	
$NO_{3_{opt}}^-$	Optimal nitrate concentration	5.0 mmol m ⁻³
$NO_{3_{width}}^-$	Nitrate concentration range	80.0 mmol m ⁻³
SR_{20}	Shoot respiration rate at 20 °C	1.0042 · 10 ⁻³ h ⁻¹
RR_{20}	Rhizome-root respiration rate at 20 °C	6.25 · 10 ⁻⁴ h ⁻¹
$V_{\max_s}^{NH_4^+}$	Shoot maximum uptake for NH_4^+	0.3 mgN gdw ⁻¹ h ⁻¹
$K_s^{NH_4^+}$	Shoot half saturation constant for NH_4^+	9.29 mmol N m ⁻³
$V_{\max_s}^{NO_3^-}$	Shoot maximum uptake for NO_3^-	0.06 mgN gdw ⁻¹ h ⁻¹
$K_s^{NO_3^-}$	Shoot half saturation constant for NO_3^-	16.43 mmol N m ⁻³
$V_{\max_r}^{NH_4^+}$	Rhizome-root maximum uptake for NH_4^+	0.02 mgN gdw ⁻¹ h ⁻¹
$K_r^{NH_4^+}$	Rhizome-root half saturation constant for NH_4^+	5.0 mmol N m ⁻³

1 Table 2. Parameters and computed quantities used in the *Ulva* model from Solidoro *et al.* (1997a) and
 2 Solidoro *et al.* (1997b).

Parameters, computed quantities	Description	Value
μ_{\max}^u	Maximum specific growth,	0.0167 h ⁻¹
$g_1(I)$	$g_1(I) = \frac{I}{I + K_I^u}$	
K_I^u	Semisaturation constant for light	239 Kcal m ⁻² d ⁻¹
$g_2(T)$	$g_2(T) = \frac{1}{1 + \exp(-\zeta(T - T_U))}$	
ζ	Temperature Coefficient	0.2 °C ⁻¹
T_U	Temperature reference	12.5 °C
$g_3(Nu)$	$g_3(Nu) = \frac{Nu - Nu_{\min}}{Nu - Nu_{\text{crit}}}$	
Nu_{\min}	Min. value for N quota	10.0 mg N/gdw
Nu_{crit}	Critical N quota level	7.0 mg N/gdw
Nu_{\max}	Max. value for N quota, uptake limitation	42.0 mg N/gdw
k_d^u	Mortality rate	6.2·10 ⁻³ h ⁻¹
k_t^u	Mortality rate due to biomass	1.0 h ⁻¹
U_{\max}	Maximum <i>Ulva</i> biomass	0.6 gdw l ⁻¹
U_{width}	Growth dependence on space availability	0.01 gdw l ⁻¹
$V_{\max_u}^{NH_4^+}$	Max. specific uptake rate for ammonium	8.5 mg N gdw ⁻¹ h ⁻¹
$V_{\max_u}^{NO_3^-}$	Max. specific uptake rate for nitrate	0.45 mg N gdw ⁻¹ h ⁻¹
$K_u^{NH_4^+}$	Half-saturation for ammonium	7.14 mmol/m ³
$K_u^{NO_3^-}$	Half-saturation for nitrate	3.57 mmol/m ³

3

4 Table 3. Parameters and computed quantities used in the phytoplankton model from Plus *et al.* (2003).

Parameters, computed quantities	Description	Value
μ_{\max}^P	Maximum specific growth,	0.021 h ⁻¹
$h_1(I)$	$h_1(I) = \left(1 - e^{-I/I_k}\right)$	
I_k	Saturation constant for light	620.1 Kcal m ⁻² d ⁻¹
$h_2(T)$	$h_2(T) = e^{\varepsilon \cdot T}$	
ε	Temperature Coefficient	0.07 °C ⁻¹
$h_3(N)$	$\frac{[NH_4^+]}{[NH_4^+] + K_N} + \frac{[NO_3^-]}{[NO_3^-] + K_N} e^{-\psi \cdot [NH_4^+]}$	
K_N	Half saturation constant for N limitation	2.0 mmol m ⁻³
ψ	Wroblewski inhibition factor	1.5 m ³ mmol ⁻¹
m_0	Mortality rate at 0 C	1.15·10 ⁻² h ⁻¹

5

6

7

8

9

10

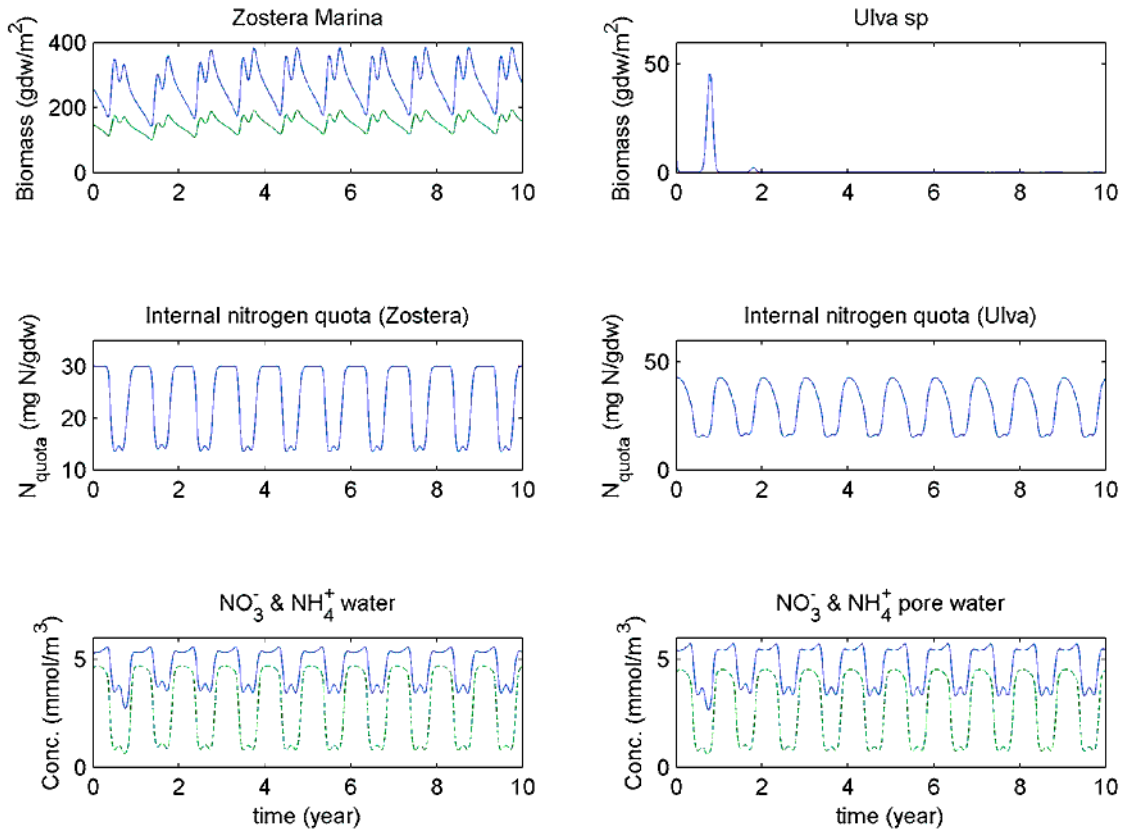
1

Table 4. Nutrient and sediment parameters, from Chapelle (1995).

Parameter s, computed quantities	Description	Value
k_{nit}	Nitrification rate at 0° C	0.0083 h ⁻¹
$f_1(T)$	$f_1(T) = \exp[k_T \cdot T]$	
k_T	Temperature increasing rate	0.07 °C ⁻¹
$f_2(O)$	$f_2(O) = \frac{[O_2]_s}{K_{NitO} + [O_2]_s}$	
K_{NitO}	Half-saturation coefficient for O ₂ limitation of nitrification	4.0 g/m ³
$RUPC$	<i>Ulva</i> stoichiometric ratio	2.5 mg P/gdw
QPS	Photosynthetic ratio	1.5
$RPHY$	Phytoplankton respiration rate at 0 C	2.083.10 ⁻³ h ⁻¹
ψ	Stoichiometric ratio	1450 g O ₂ /gdw
RPS	O ₂ produced/N	0.212 g O ₂ /mmol
D_{NO}	Diffusion coefficient for nitrate in the sediment	0.00072 m ² /h
D_{NH}	Diffusion coefficient for ammonium in the sediment	0.00072 m ² /h
A	Surface of computationa cell	1 m ²
z_S	Distance between the centre of water cell and sediment layer	0.51 m
$watervol$	Volume of the water cell	1 m ³
$interstvol$	Interstitial water volume for a cell	0.008m ³
k_{denit}	Denitrification rate at 0° C	0.0125 h ⁻¹
$f_3(O)$	$f_3(O) = 1 - \frac{[O_2]_s}{K_{denitO} + [O_2]_s}$	
$[O_2]$	Oxygen concentrarion	8 g/m ³
K_{denitO}	Half-saturation coefficient for O ₂ limitation of denitrification	2.0 g/m ³
α_{denit}	percentage of N denitrified into N ₂	0.6
$f_4(O)$	$f_4(O) = \frac{[O_2]_s}{K_{minO} + [O_2]_s}$	
K_{minO}	Half-saturation coefficient for O ₂ limitation of mineralization	0.5 g/m ³

2

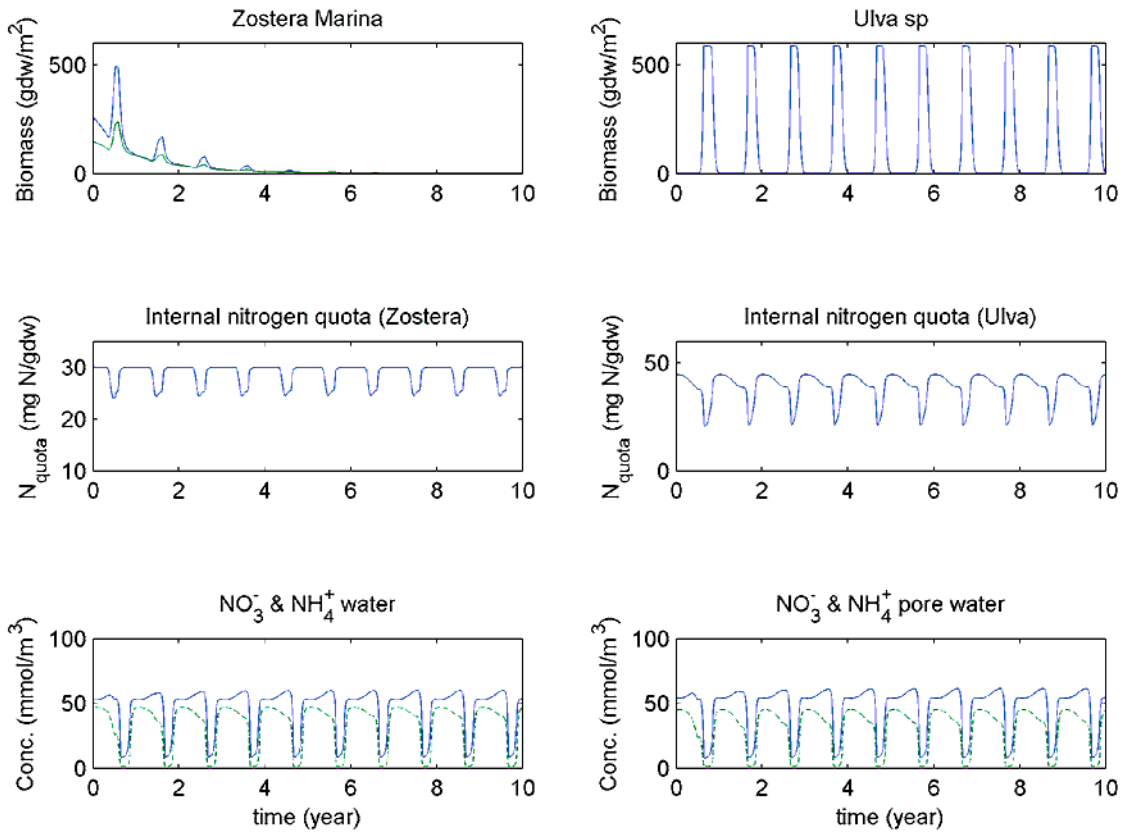
3



1

2 Figure 1. *Zostera* biomasses Z_s (shoot biomass, gdw m^{-2}) and Z_r (rhizome-root biomass, gdw m^{-2} -in
 3 green-); *Ulva* biomasses (gdw m^{-2}); Internal nitrogen quotas; DIN concentrations (NO_3^- : blue, NH_4^+ :
 4 green) in the water column and in the sediments (pore water). $F = 0.1 \text{ m}^3 \text{ h}^{-1}$, and
 5 $[\text{NO}_3^-]_{input} = [\text{NH}_4^+]_{input} = 5 \text{ mmol m}^{-3}$ (low nutrient situation).
 6

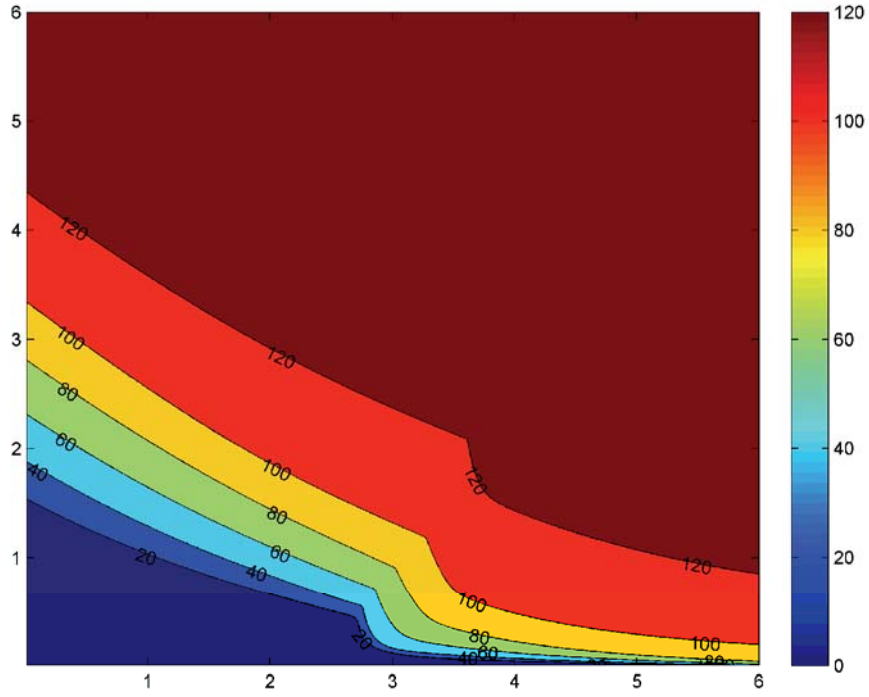
1



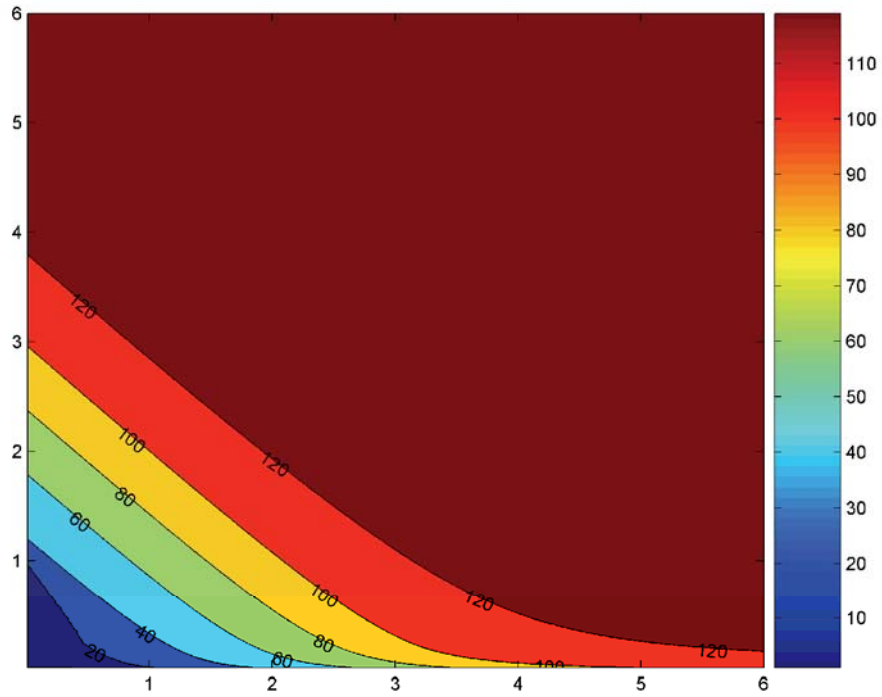
2

3 Figure 2. *Zostera* biomasses: Z_s (shoot biomass, gdw m^{-2}) and Z_r (rhizome-root biomass, gdw m^{-2} -in
 4 green-); *Ulva* biomasses (gdw m^{-2}); Internal nitrogen quotas; DIN concentrations (NO_3^- : blue, NH_4^+ :
 5 green) in the water column and in the sediments (pore water). $F = 0.1 \text{ m}^3\text{h}^{-1}$, and
 6 $[\text{NO}_3^-]_{\text{input}} = [\text{NH}_4^+]_{\text{input}} = 50 \text{ mmol m}^{-3}$ (High nutrient situation).
 7

1



2



3

4

5

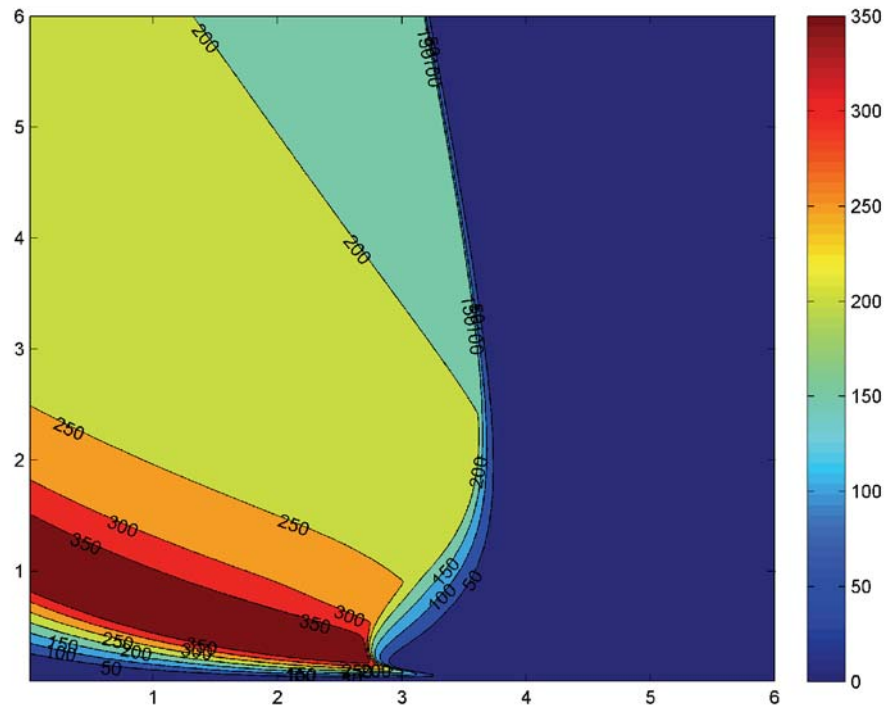
6

7

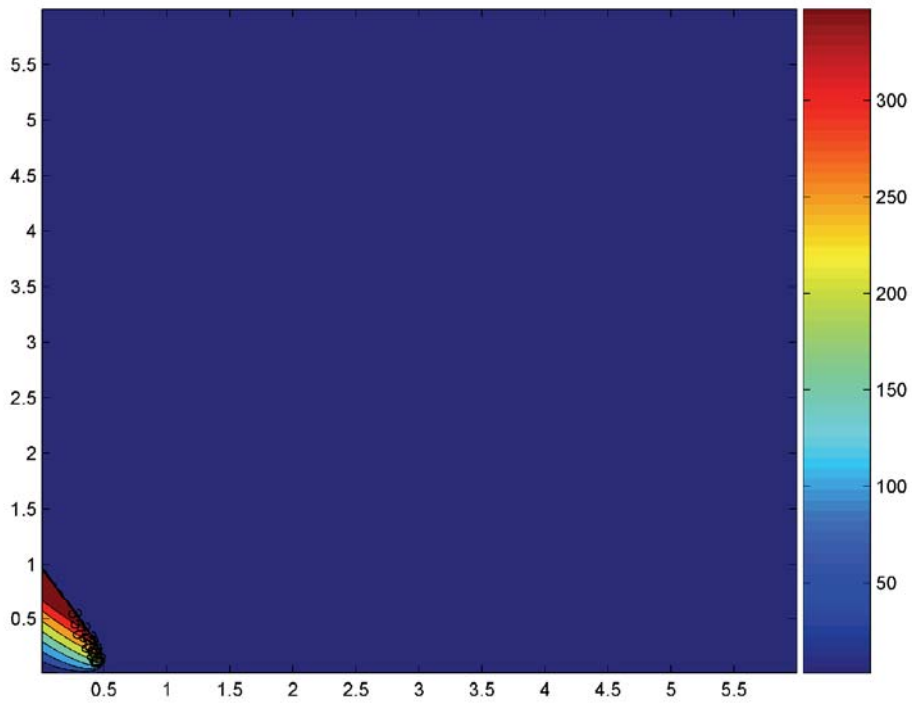
8

Figure 3. *Ulva* annual mean biomass (gdw m⁻²) as a function of nitrate (x-axes) and ammonium loads (y-axes) in mmol h⁻¹. Top: $F=0.1 \text{ m}^3 \cdot \text{h}^{-1}$; bottom: $F=0.01 \text{ m}^3 \cdot \text{h}^{-1}$.

1



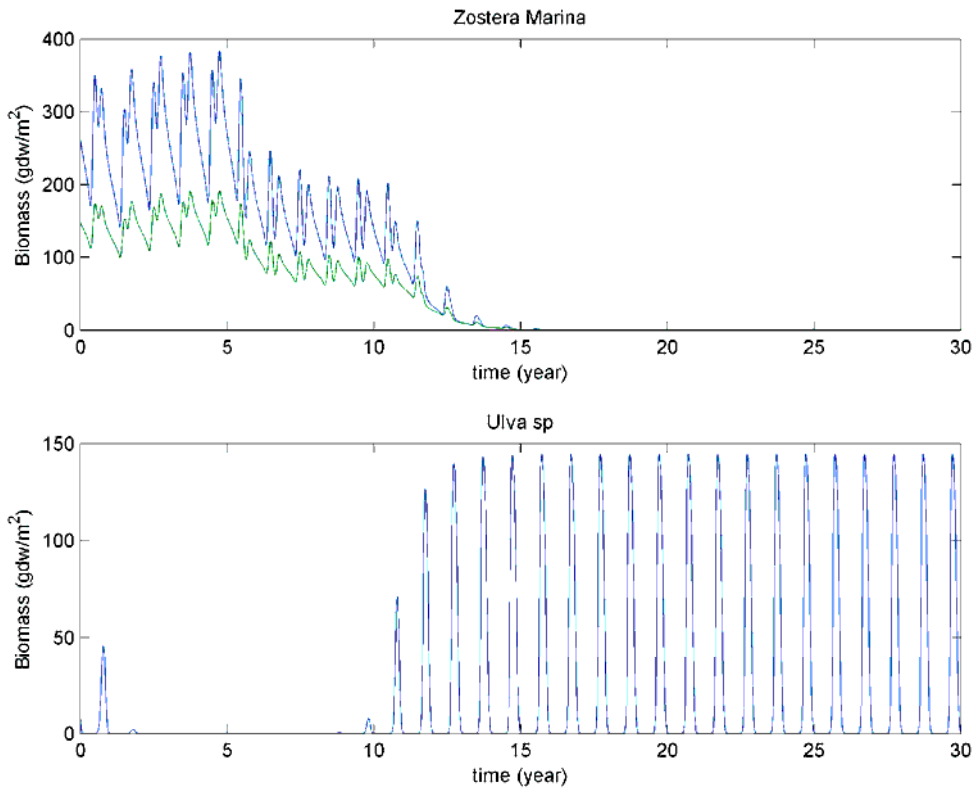
2



3

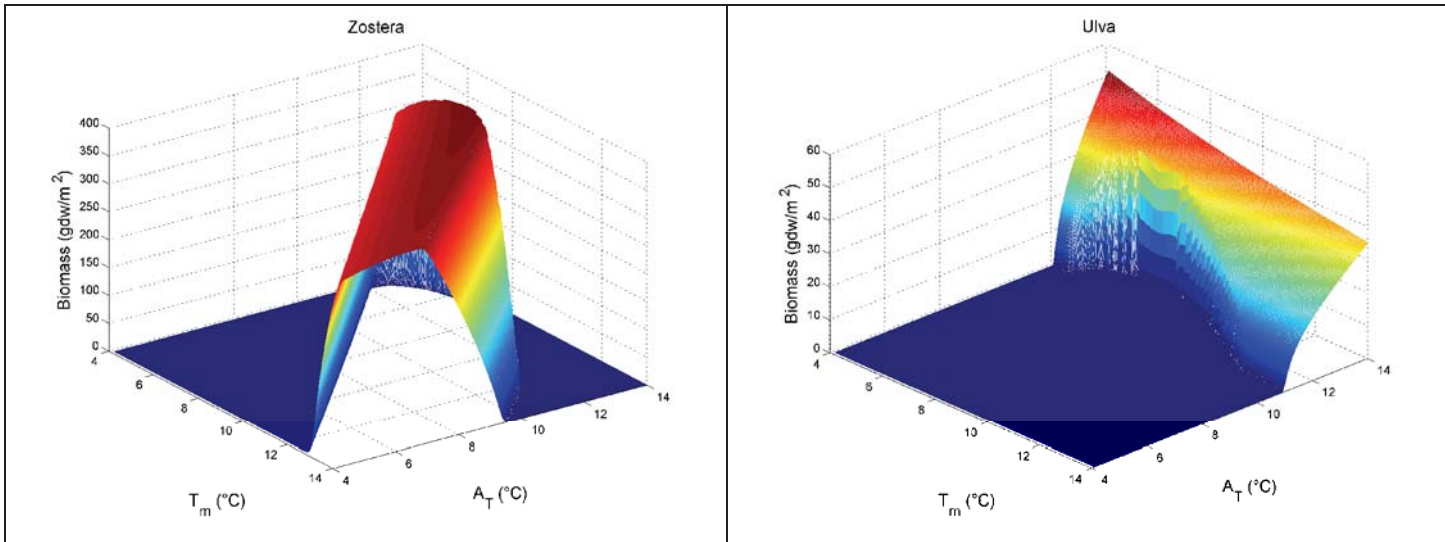
4 Figure 4. *Zostera* annual mean biomass (gdw m⁻²) as a function of nitrate (x-axes)
5 axes) loads in mmol h⁻¹. Top: $F=0.1 \text{ m}^3 \cdot \text{h}^{-1}$; bottom: $F=0.01 \text{ m}^3 \cdot \text{h}^{-1}$.

6



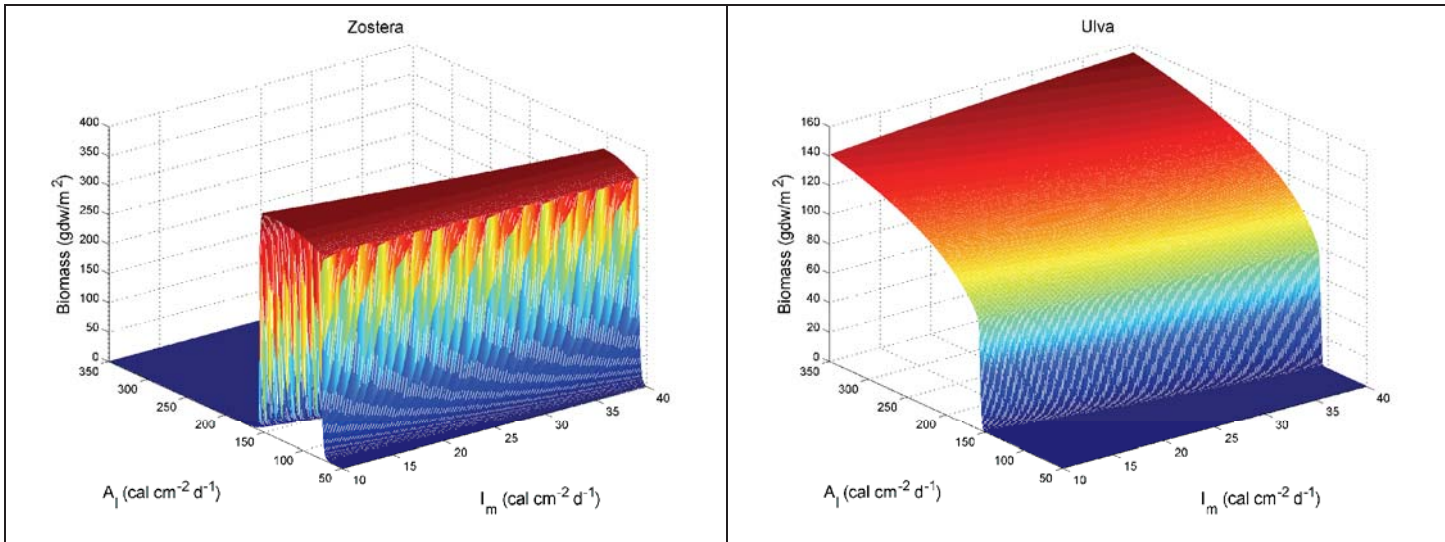
1
 2 Figure 5. *Zostera* biomasses: Z_s (shoot biomass, gdw m^{-2} , blue) and Z_r (rhizome-root biomass, gdw m^{-2} , green) and *Ulva* biomasses (gdw m^{-2}). Same parameters as in Fig. 1, but after the fifth year of
 3
 4 simulation the temperature forcing function increases by 1.0°C .
 5
 6

1



2 Figure 6. *Zostera* and *Ulva* annual mean biomass (gdw m⁻²) as a function of mean temperatures, T_m ,
3 and its amplitude of annual variation, A_T , for the low nutrient regime, $F=0.1$ m³h⁻¹ and
4 $[NO_3^-]_{input} = [NH_4^+]_{input} = 5$ mmol m⁻³.
5

1



2 Figure 7. *Zostera* and *Ulva* annual mean biomass (gdw m⁻²) as a function of mean light intensity, I_m ,
3 and its amplitude of annual variation, A_l , for the high nutrient regime, $F=0.1 \text{ m}^3 \text{ h}^{-1}$ and
4 $[NO_3^-]_{input} = [NH_4^+]_{input} = 50 \text{ mmol m}^{-3}$.

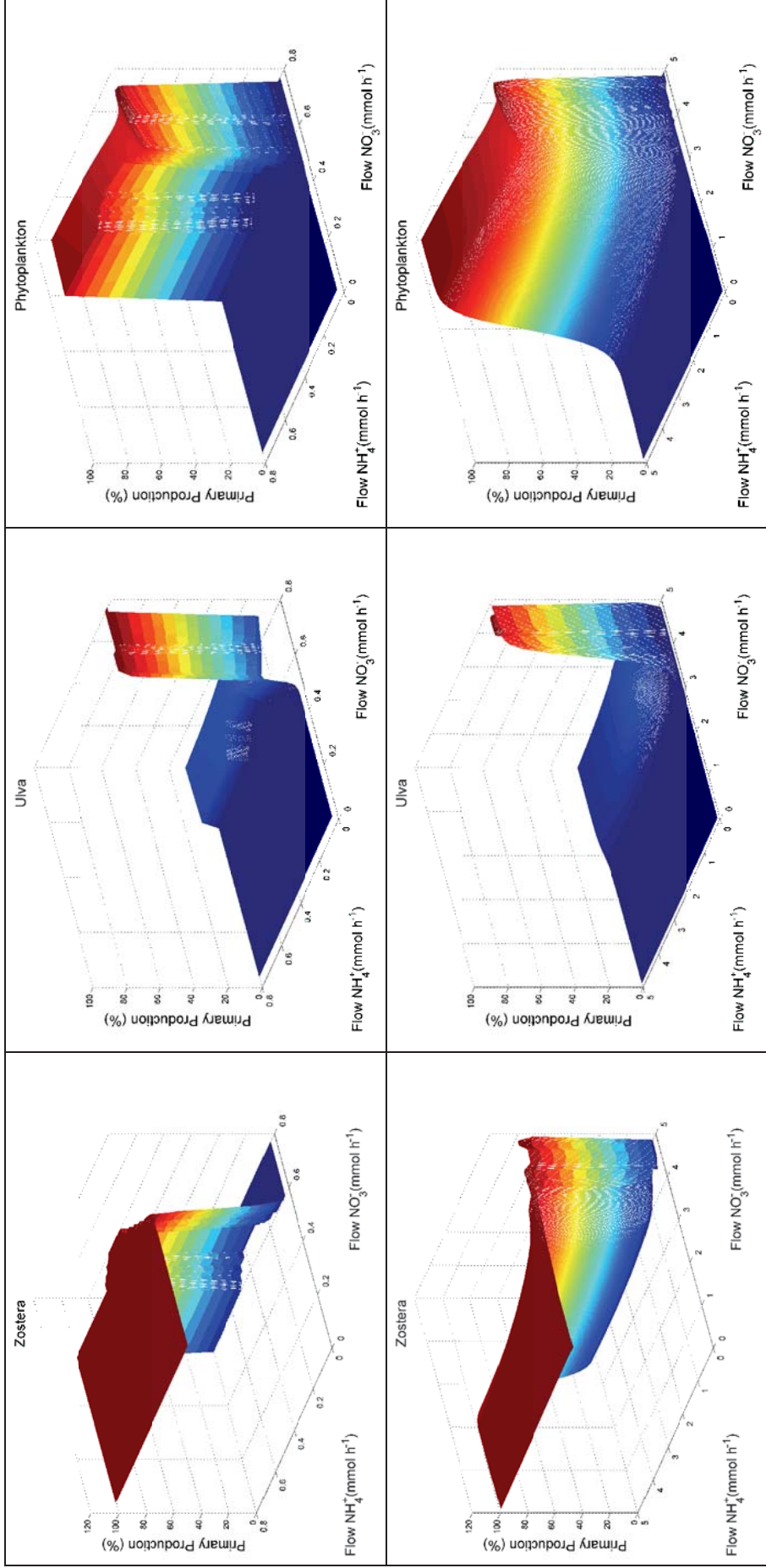


Figure 8. Percentage of primary production for each compartment: *Zostera*, *Ulva* and phytoplankton as a function of nutrient flows. Top: $F=0.01 \text{ m}^3 \text{ h}^{-1}$; bottom: $F=0.1 \text{ m}^3 \text{ h}^{-1}$.

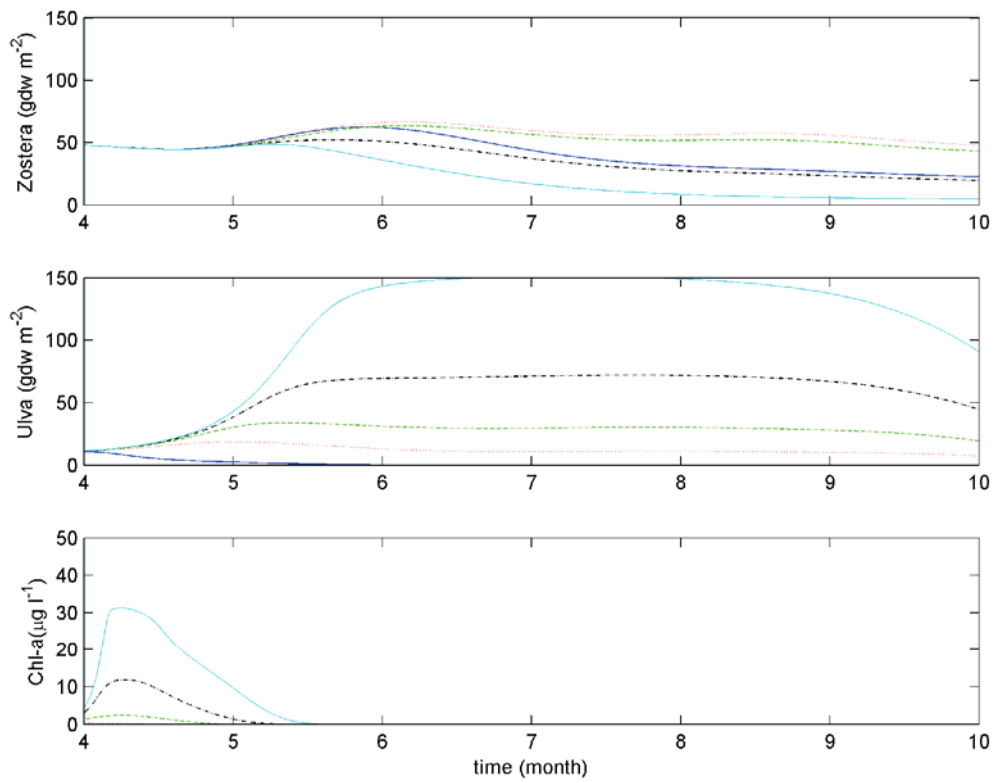


Figure 9. Simulated biomasses of *Zostera*, *Ulva* and phytoplankton during the mesocosm experiments from Taylor et al. (1999). Control (C): continuous blue line; Low (L): dotted red line (L); Medium (M): dashed green line; High (H): dash-dot black line; Very high (VH): continuous cyan line.

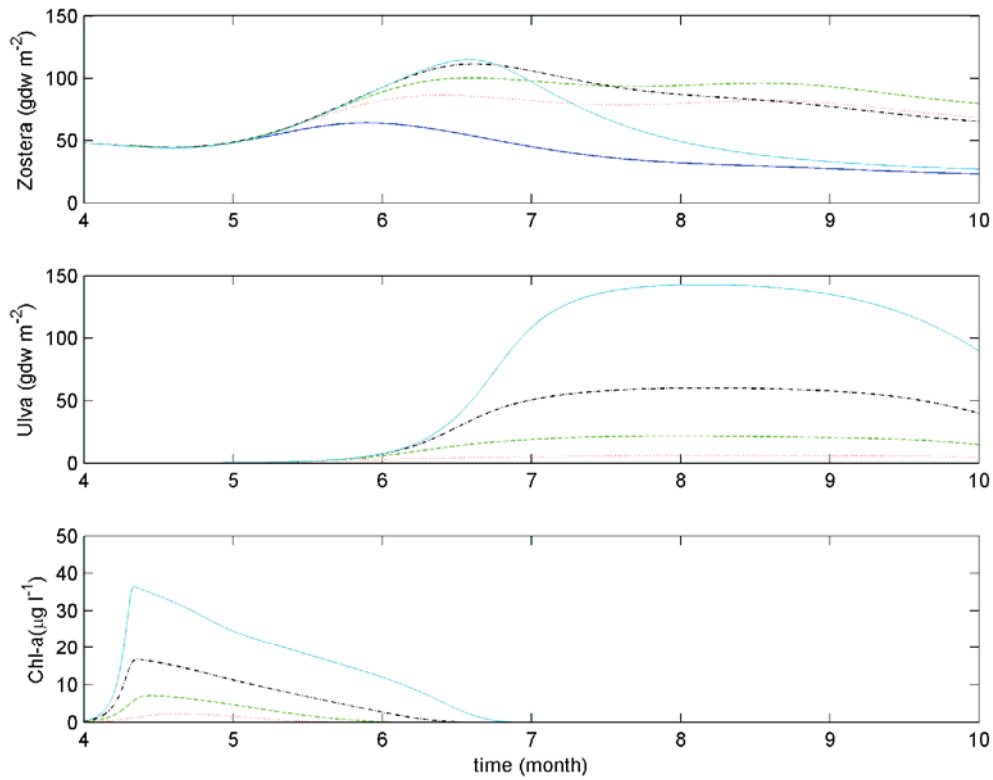


Figure 10. Simulated biomasses of *Zostera*, *Ulva* and phytoplankton during the mesocosm experiments from Taylor et al. (1999). Control (C): continuous blue line; Low (L):dotted red line(L); Medium (M):dashed green line; High (H): dash-dot black line; Very high (VH): continuous cyan line. Conditions as Fig. 9 but the initial conditions of *Ulva* and phytoplankton have been reduced by a factor of ten.